International Journal of Advanced Trends in Computer Applications
www.ijatca.com

Transient CFD analysis of Hull Shape of Autonomous Underwater Vehicle based on Minimization of Drag force on it & structural analysis of the optimized shape

[1]Tanumoy Banerjee, [2]Nripen Mondal, [3]Md. Naim Hossain
[1,2,3] Department of Mechanical Engineering,
Jalpaiguri Government Engineering College, Jalpaiguri-735101, West Bengal, India
[1]Tanumoybanerjee88@gmail.com, [2]nripen_mondal@rediffmail.com, [3]naimhossain6@gmail.com

Abstract: *An autonomous underwater vehicle (AUV) is an unmanned (i.e. without requiring input from an operator) underwater self-propelled robot. They are a part of a larger class of unmanned underwater vehicles of which another part is Remotely Operated Vehicles (ROVs). AUVs are programmed at the surface, then navigate through the water on their own and collect data as they go. As against AUVs, ROVs remain tethered to the host vessel and controlled and powered by an operator through an umbilical. In this paper investigation of the hull shape of the AUV has been design based on the minimisation of Coefficient of Drag. The present AUV model has been prepared considering 2D axisymmetric geometry in ANSYS Fulent-16. As the computer technology developed very rapidly, computational fluid dynamics (CFD) is now widely applied to analysing AUV hydrodynamic performance. In our venture, we are using SolidWorks for modelling and ANSYS for simulation. The CFD analysis provides better drag estimates over the empirical ones and also provides accurate stimulations of the flow around the vehicles. The paper is configured in two phase. Initially, the investigation done in shape of the nose and tail with unstructured meshing with SST k-ω model by comparing different types of shape with their corresponding Coefficient of drag value. The optimized shape is then used to produce a 3D body, which is subjected to structural analysis in ANSYS 16.0. Stress concentration is inspected for varying depth of the submerged AUV.*

Keywords: Autonomous Underwater Vehicle(AUV), Coefficient of Drag, SST k-ω model, Simple Scheme

I. INTRODUCTION

AUV is used now a day in many marine activities. However, effective utilization of CFD for marine hydrodynamics depends on proper selection of turbulence model, grid generation and boundary resolution. For energy utilization and endurance improvement, it is necessary to optimize AUV hulls on the basis of correct drag estimation. Here research is based on the Reynolds Averaged Navier–Stokes (RANS) formulation because these equations can be used to model the flow turbulence model for the hull shape to give time-averaged solutions of Navier–Stokes equations for momentum (Ting, 2016). The RANS equations are primarily used to describe turbulent flows & for this the viscous effects are much better than potential flow theory and needs less computer resources than large eddy simulation (LES) (Ting, 2016). Stevenson (2007) compared the drag performance of seven representative revolution bodies which were all scaled to the same volume. The results suggest that a laminar flow body form could be more efficient than a torpedo form, but it was more sensitive to ancillaries and manufacturing imperfections. The application of formal optimization methods to the drag minimization or to evaluate optimum design of AUVs have not gained much attention by the researchers so far (Parsons, 1974). It is important to highlight that the use of efficient optimization tools leads to better product quality and improved functionality (Diez, 2010). Moonesan (2015) also made a comparison among four hull forms and found that two of the forms have superior drag performance compared to the other two. In this paper, Optimization is done on the hull shape of Nose and tail from though standard equation in axisymmetric model. CFD can offer a cost-effective solution to the above problem (Karim, 2008). CFD is becoming more popular due to availability of commercial software (Karim et al. 2008, Tyagi et al., 2006, Tang et al., 2009). Structured meshing has definite mesh relation and it give most accurate result. For optimising, unstructured meshing is suitable concerning about time saving prospective. The CFD simulation has been employed in, Fluent (ANSYS 16), ICEM CFD, Mesh Modeller, surface of the flow domain has been modelled in the Solid Works (2013) & graphs are plotted in Origin Pro Software. SST k-ω model is used for turbulence simulation in Fluent 16.

II. HYDRODYNAMIC MODULE

a) Drag Estimation

Drag (also called fluid resistance) is a that arises due to the relative motion between an object and its surrounding flow field that acts in the opposite direction of the motion of the moving object. In hydrodynamics of a AUV we come across two types of drags viz. Pressure Drag and Viscous Drag. Summation of these two quantities gives the value of total drag experienced by the AUV. Optimization of hull shape is done through minimization of drag force which eventually reduces the power requirements of the AUV. For estimation of total drag, the following formula is used,

$$D = \frac{1}{2}\rho v^2 C_d A_w \qquad (1)$$

b) Wall Shear Stress

Wall shear stress can be determined from the velocity profile of the boundary layer. Knowing what the wall shear stress is, will make it possible to determine the part of the drag forces that could be acting on the submerged vehicle. To calculate the wall shear stress using the Blasius equation given by,

$$\tau_w = 0.332 v^{1.5}\sqrt{\frac{\rho\mu}{x}} \qquad (2)$$

c) Skin Friction Coefficient

Skin friction coefficient is determined by the ratio of wall shear stress and dynamic pressure of a free stream. It is given by,

$$C_f = \frac{\tau_w}{0.5\rho v^2} \qquad (3)$$

III. MATHEMATICAL MODEL

a) Theoretical Formulation

For the flow past an axi symmetric underwater vehicle hull form, the continuity equation in cylindrical co-ordinate is given by,

$$\frac{\partial\rho}{\partial t} + \frac{\partial}{\partial x}(\rho v_x) + \frac{\partial}{\partial r}(\rho v_r) + \frac{\rho v_r}{r} = S_m \qquad (4)$$

where x is the axial co-ordinate, r is the radial co-ordinate, v_x is the axial velocity, v_r is the radial velocity and S_m is the source term (taken as zero in this study). The axial and radial momentum equations are given by,

$$\frac{\partial}{\partial t}(\rho v_x) + \frac{1}{r}\frac{\partial}{\partial x}(r\rho v_x^2) + \frac{1}{r}\frac{\partial}{\partial r}(r\rho v_r v_x) = -\frac{\partial p}{\partial x} + F_x \qquad (5)$$

$$\frac{\partial}{\partial t}(\rho v_r) + \frac{1}{r}\frac{\partial}{\partial x}(r\rho v_x v_r) + \frac{1}{r}\frac{\partial}{\partial r}(r\rho v_r^2) = -\frac{\partial p}{\partial r} + F_r \qquad (6)$$

where p is the static pressure and F is the external body force (taken as zero here) and,

$$\nabla . v = \frac{\partial v_x}{\partial x} + \frac{\partial v_r}{\partial r} + \frac{v_r}{r} \qquad (7)$$

Total viscous drag, $D = D_f + D_p$

$$D_f = 2\pi\int_0^{X_e} r_w \tau_w \cos\alpha \, dx \qquad (8),$$

$$D_p = 2\pi\int_0^{X_e} r_w p \sin\alpha \, dx \qquad (9)$$

b) Geometrical Formulation

A typical AUV consists of three parts i) nose (bow) ii) middle body & iii) tail (stern or aft). The hull middle body is of cylindrical shaped & the modified semi elliptical profile equation for the nose (as per Myring type body). Here the optimization is done firstly for nose shape i.e., various nose shapes are simulated keeping the tail fixed & later (2) e optimised nose shape various tail shapes are ed & finally the optimised total hull shape is obtained. Axis symmetric body of revolution moving submerged near to the free surface is considering in this paper. Total body length of l units, a+b+c=1=l, the nose radius, r_n has been taken from Ting et al., 2016

$$r(x) = \frac{d}{2}[1 - \left(\frac{x-a}{a}\right)^2]^{\frac{1}{n}}$$

There are two variables, length of nose *a* and the index *n*. We have followed the following steps for reaching the desired shape for minimal drag.

Table 1: Range of parameters a & n for design consideration (Ting et. al, 2016)

Parameter	Minimum	Maximum
a	0.5d	1600 mm
n	0.6	3.0

The tail profile is taken based on the following curve (based on Ting et al., 2016)

$$r(x) = \frac{d}{2} - \left(\frac{3d}{2c^2} - \frac{tan\theta}{c}\right)(x - a - b)^2 + \left(\frac{d}{c^3} - \frac{tan\theta}{c^2}\right)(x - a - b)^3$$

After the optimization of the nose shape, we come to a conclusion that the variation of the nose index n while keeping a fixed, is less significant than the variation of a while keeping n fixed. So, we have to change n as well as a at the same time for reaching the optimized shape for the nose. By doing this, we find that the drag force becomes minimum when we take *n=2.05* & *a=235*.

We simulated the various different tail shapes by varying the variables θ & c to check for which shape the drag as well as the turbulent kinetic energy & energy losses due to eddy formation becomes the minimum. Thus, we find that for the shape for c=504, θ=30° we get the minimum drag, turbulent K.E & minimum energy losses due to eddy formation.

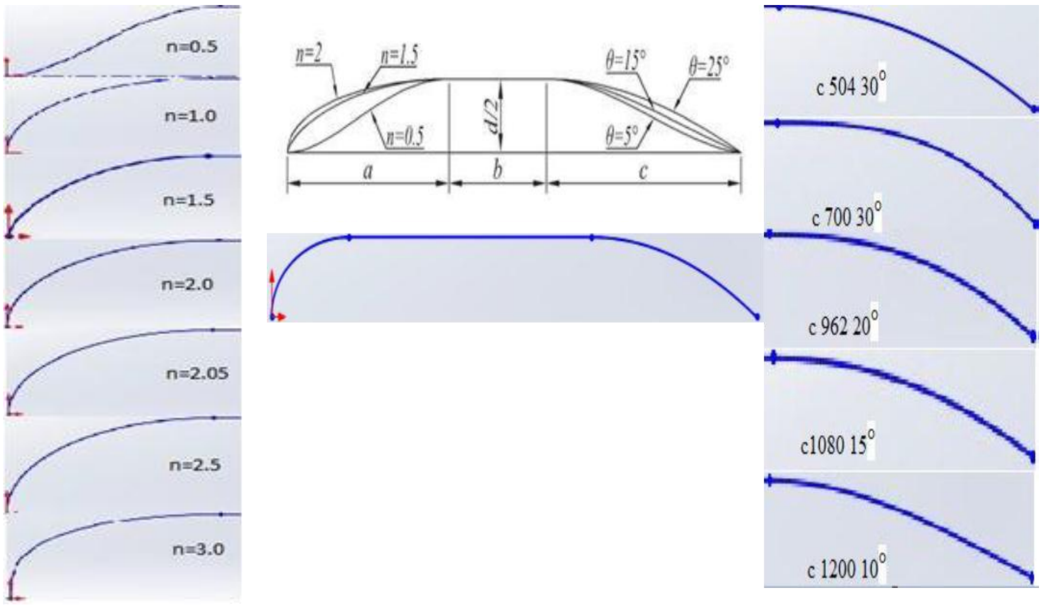

Figure 1: Various nose shapes simulated for drag minimization (left), Actual Schematic View of hull shape with all notations given (middle top), Various different tail shapes simulated keeping the optimised nose shape as fixed (right), Final optimised shape of hull (middle bottom)

c) Numerical Domain, Mesh Generation & Adopted Numerical Schemes

With regard to the relativity of motion the flow past a stationary body is simulated instead of moving bodies in still water in order to enhance calculative efficiency. 2D numerical domain (Ting, 2016) is created which comprises only a half middle section plane with the upper half of the hull boundary. The length of the domain is 15 times the length of the body, the nose is at a distance of 5 times the body length from the velocity input surface and 10 times the body length from the velocity output surface. The width of the domain is about 25 times the radius of the cylindrical middle section of the hull. The numerical domain along with the created part is as follows (Ting, 2016).

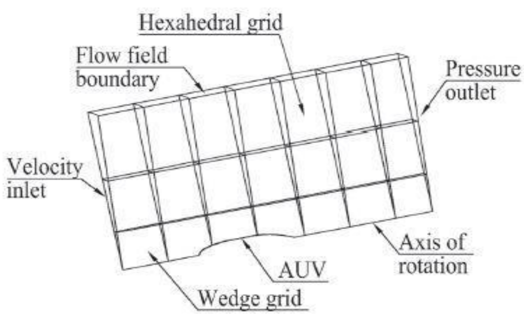

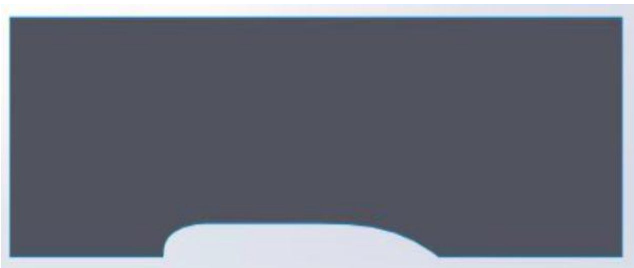

Figure 2: Schematic View of Numerical Domain (left), Actual Numerical Domain Created for simulation (right)

Meshes are generated using the *Mesher* tool available in the *ANSYS Workbench v16.0*. Triangular meshes are generated. Total number of cells and nodes are 32661 and 26775 respectively. Bias factor of 20 is taken for sizing of the nose and tail edge meshes with relevant bias types. 50 inflation layers are imposed on the hull boundary to get fine meshing.

The commercial software ANSYS Fluent is selected as the CFD solver. The Reynolds' averaged Navier Stokes (RANS) equations that solve time-average mass and moment conservation equations are used as the basis for conduction the numerical calculations. In the Fluent launcher double precision method is selected along with parallel computation. Governing equations, underlying the assumptions of incompressible, isothermal and transient are solved on the basis of finite volume method. A k-ω shear stress transport (k-ω SST) turbulence model is employed. The SST k-ω turbulence model is a two-equation eddy viscosity model which effectively blends the robust and accurate formulation of the k-ω model in the near wall region with the free stream independence of the k-ϵ model in the far field. SST model blends k-ω & k-ϵ model in the boundary zone. The coupling between pressure and the velocity fields is achieved using SIMPLE scheme. A second order upwind is used for both turbulence kinetic energy and specific dissipation rate. A second order implicit transient formulation is employed. In the solution force monitor we created the drag print & plot to show the drag force generated versus time of flow. Hybrid initialization is chosen for initialization and a time step of 0.001s along with 1000-time steps is taken.

IV. RESULTS

The simulation is done with fluid flow velocities ranging from 0.3 m/s up to 2.1 m/s with an increment of 0.2. The various contours & plotted graphs for the average velocity of the AUV of v=1.7 m/s are shown below.

a) Generated Plots

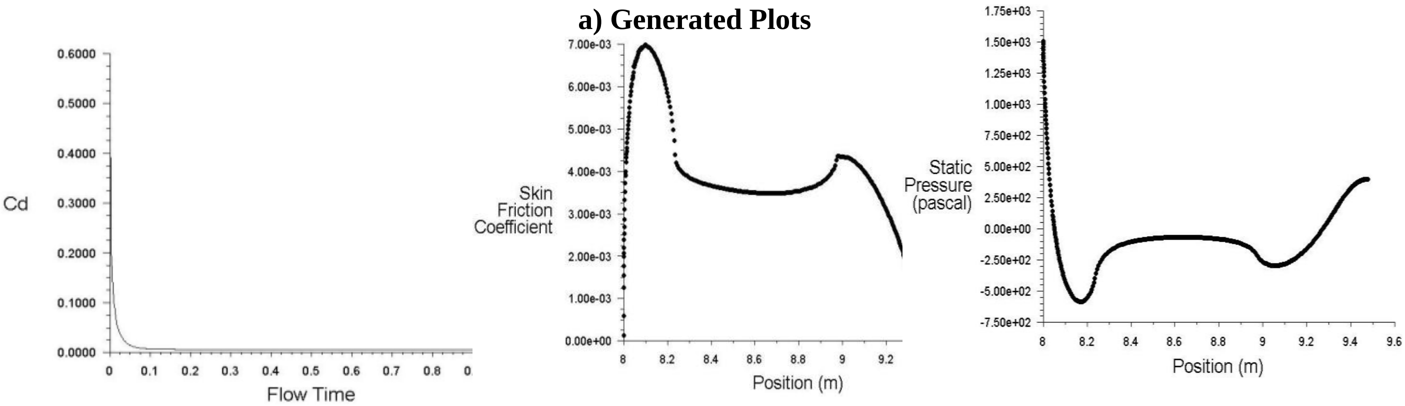

Figure 3: Drag Convergence plot with flow time for velocity v=1.7 m/s (left), Skin friction coefficient vs Hull length (in metre) plot for velocity 1.7 m/s (middle), Static Pressure (in Pascal) vs Hull length (in metre) plot for velocity 1.7 m/s

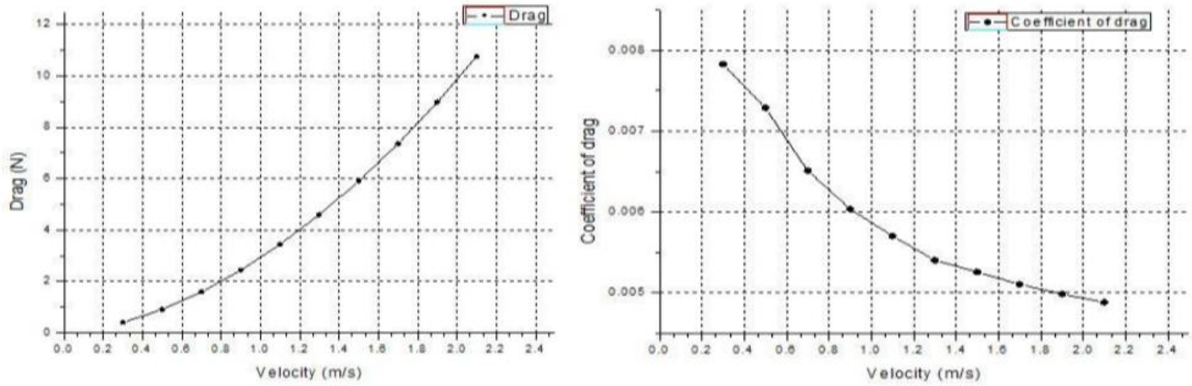

Figure 4: Drag vs Velocity (left) & Coefficient of drag vs velocity graph for various velocities

b) Generated Contours

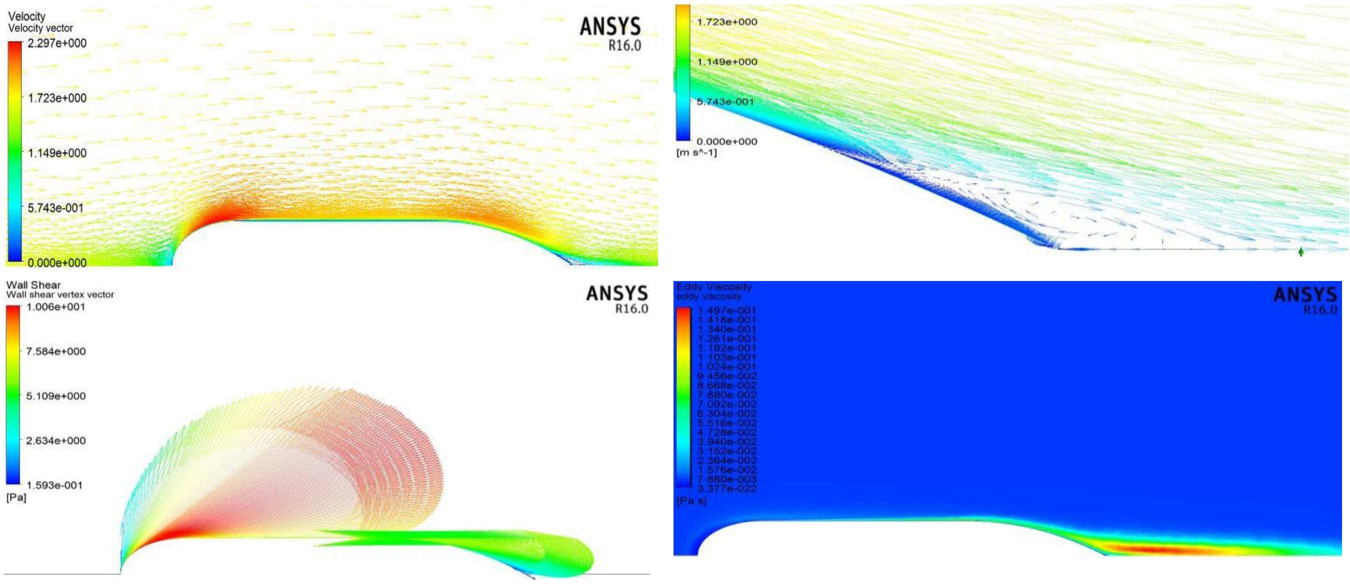

Figure 5: Velocity Vector around the hull (top left), Formation of eddies shown (top right), Wall shear stress along the hull length (bottom left), Turbulent eddy viscous force effect (bottom right)

Here the velocity vector profile is shown along the length of the hull. Formation of eddies & for this the amount of turbulent kinetic energy is lost which is also shown in velocity contours. Turbulent eddy viscosity effect is found maximum after the tail edge & turbulent eddy dissipation rate is very minimum near the hull shape. Wall shear stress vector is shown. As the velocity of fluid becomes zero on the hull surface due to selection of no slip boundary condition, wall shear stress just at the tip of the nose is found to be the minimum & due to sudden rise in fluid velocity after the nose length, wall shear stress have a parabolic increase in nature (from equation 2) & also at the end of tail, due to formation of eddies shear stress is found negligible. As we know that power requirement of an AUV is thoroughly dependent on the amount of drag force (pressure & viscous) acting on the nose & amount of turbulence created due to formation of eddies after the tail section where some kinetic energy is lost, so the optimization of the hull profile for minimum drag & min TKE is one of the basic requirements for proper utilization of available power to run the AUV.

V. STRUCTURAL ANALYSIS OF OPTIMISED SHAPE OF HULL

Here we will discuss about the stress concentration and behaviour of the structural model of AUV at different depths. Half portion of the hull is modelled for the simplicity of analysis. 3D shape is generated using the optimized hull shape discussed in the previous sections. Thickness of the model is assumed to be 20mm. The material chosen is alister 3000 (Mahendra, 2013). The typical chemical composition of the material is 0.565 carbon, 1.8% Si, 0.7% Mn, 0.045% P, & 0.045% S.

Table 2: Mechanical Properties of material used for structural analysis

Properties	Value
Density	7860 kg/m^2
Young's Modulus	2.1e5 N/mm^2
Poisson's Ratio	0.3
Yield Strength	500 N/mm^2
Tensile Strength	620 N/mm^2

For the current analysis, we have chosen tetrahedral element. This element supports structural analysis, linear and non-linear. All the areas of the model have been modelled with the same element. Element size is taken as 5mm. The numbers of nodes are 114308 and that of elements are 63282. The hydrostatic pressure due the weight of the water around the AUV is to be applied. As we know that hydrostatic pressure varies linearly with depth of fluid i.e.,

$$P=\rho gH$$

where ρ is the density of water, g is the acceleration due to gravity and H is the depth at which the AUV is submerged. Here the analysis is done at varying depths-20 m to 200 m with an increment of 20 m.

Table 3: Symmetric & Applied boundary considerations of the shape

	Degrees of Freedom					
Plane	X	Y	Z	RX	RY	RZ
X=0	0	F	F	F	0	0
Y=0	F	0	F	0	F	0
Z=0	F	F	0	0	0	F

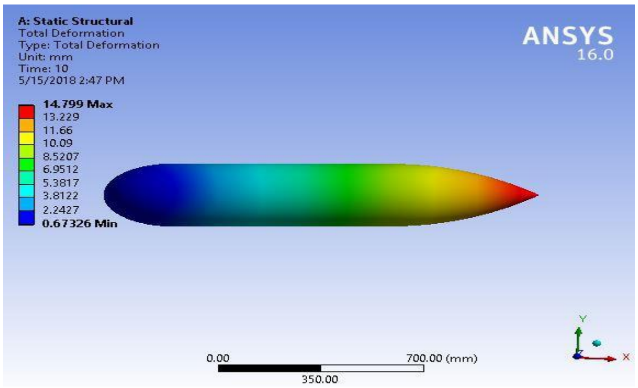

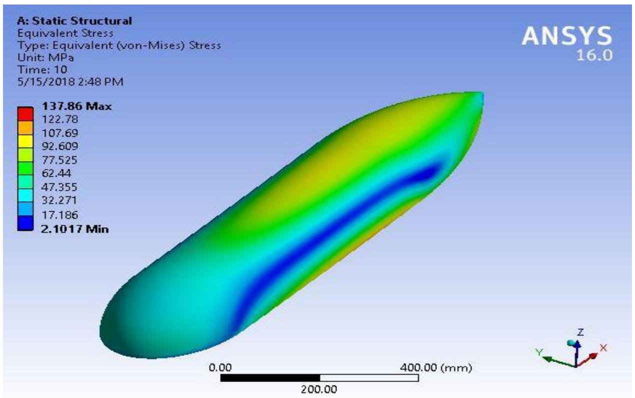

Figure 6: Total deformation contour for 3D hull shape (left), Equivalent Stress (Von-Mises) contour for 3D hull shape (right)

Here, the static structural analysis is done to check how much hydrodynamic pressure the optimized hull can resist while in operation underwater. Total deformation contours are generated to find out how much the body of hull is deforming under that condition, we found out that maximum total deformation of 14.8 mm is observed at tail end section & minimum of 0.6 mm is observed at nose tip for the optimized shape. Equivalent or Von-Mises stress is calculated over the domain to check how much stress the bare hull is experiencing & depending on that selection of proper hull material & design can be conducted. A maximum of 137.86 MPa stress is found in upper half & at tail of the hull body which can be minimized by using ribs, composite materials.

VI. DISCUSSION

Table 4: Different values of coefficient of drag, total drag for different types of meshing

Meshing Type	C_d (x10^{-3})	C_p (x10^{-3})	D_f (N)	D (N)
Structured Mesging	2.52	0.415	2.65	3.26
Unstructured Meshing	3.48	0.403	3.02	3.61

From the above table, it is seen that that there is a variation in the value of C_d and C_p in two types of meshing. But structured mesh shows accurate relation between the cell zone. From here it is also clear, there is a variation of C_d for both type of meshing with the variation of no of cells but there always exists a clear difference in the value of C_d in simulated in same environment and in same no of edge discretization near tail and nose. It means refinement can be done to some extent but due to limited computer resources the solution is stopped. But it is found out that with same no of cells, structured meshing gives lowest value of C_d. The simple algorithm make the solution converges by giving a suitable relation between the cell which is connected suitably with proper mesh relation, that why it is taken close to the actual result. By this how the variation in vale is occur with mesh configuration is shown. The pressure coefficient value in fig. 3 reduces at the leading nose edge after which increases in the mid-section and becomes constant throughout the parallel middle body. Close to after body the curve dips for a while and moves up at the trailing edge. The curve of the wall shear stress and skin friction coefficient in fig. 3 has the same tendency like increasing at nose then dips and shows less variation at middle then increases at tail junction and finally decreases. At the tail section due to boundary layer separation & due to eddy formation large amount of kinetic energy is lost & thus the shear stress increases further there at the trailing edge. The graphs plotted in fig. 4 shows that with increase in velocity the drag force increases in spite of the coefficient of drag decreases because their viscous drag increases thus total drag force increases. Wall shear stress contour is given in fig. 5 and for the structural analysis part total deformation contour & equivalent von-mises stress contours are given & according to these the thickness is to be determined.

VII. CONCLUSION

In this paper an optimized platform for AUV hull shape is presented. Here an unstructured 2D mesh, standard wall function and adaptive mesh strategy are applied for calculating the drag of bodies of revolution. Its use can greatly improve computational efficiency. Power requirements of an AUV directly depend upon the drag resistance. Thus, the optimized hull shape designed by minimization drag will increase the operational efficiency of the AUV. According to the optimization results, the traditional AUV hull shape with a long cylinder as the middle part is not a good option for drag reduction. Shape of AUV optimisation is one of important part of the research field. This paper gives framework to further study in the field of AUV to decrease the drag for improving the power consumption and speed of AUV in underwater condition. This paper gives a very brief idea how the index, angle in the equation vary with drag. The structured and unstructured result show how mesh quality effect the result.

The aim of the structural analysis was done for checking if that model can withstand sea pressure at depth. Studying the stress analysis, we can say that this hull can operate in shallow depths (100-200m). Beyond that the hull is subjected to high stresses and high displacement. We can observe high deformation at the tail section which can be minimized by using composite material for making the tail. The stress can be minimized at for greater depths by providing reinforcements such as ribs and vertical plates can be used to decrease stresses, T-beams is effective where displacements are high, and lastly the design of the hull can be optimized more for this purpose. High accuracy and further optimization of the hull shape can be obtained using various optimizer software. For the structural analysis, a buckling analysis allows to know accurately the limit of depth and which critical loads bring to failure. Moreover, the model using non-linear condition will give better results for stress past yield stress. A modification of the hull thickness can be tested through a buckling analysis.

Conflict of Interest

All authors have equal contribution in this work and declare that there is no conflict of interest for this publication.

Acknowledgement

The author(s) would like to acknowledge the esteemed support and guidance from Department of Mechanical Engineering at Jalpaiguri govt. engg. College to carry out the present study. It is a project conducted in our college & experimental set up is being built to check the case with numerical & analytical solution.

References

[1]. Diez M. and Peri D., Robust optimization for concept ship design, *Ocean Engineering*, vol. 37, pp. 966–977, 2010.
[2]. Karim M. M., Rahman M. M., and Alim M. A., Numerical Computation of Viscous Drag for Axisymmetric Underwater Vehicles, *J. Mekanikal,* vol. 26, pp. 9–21, Dec. 2008.
[3]. Mahendra B., Ankanna B., Tirupathi K. Reddy & Ravichandra M., *International Journal of Modern Engineering Research (2013)*
[4]. Moonesun M., Mikhailovich K. Y., Hosein D., CFD Analysis on the Bare Hull Form of Submarines for Minimizing the Resistance, *IJMT Vol.3/winter/2015(1-16)*
[5]. Parsons J. S., Goodson R. E., and Goldschmied F. R., Shaping of Axisymmetric Bodies for Minimum Drag in Incompressible Flow, *J. Hydronautics, vol. 8, no. 3, pp. 100–107, 1974*
[6]. Stevenson P., Furlong. M. & Dormer D., AUV shapes - combining the practical and hydrodynamic considerations. *OCEANS 2007- Europe*.
[7]. Tang S., Ura T., Nakatani T., Thornton B., and Jiang T., Estimation of the hydrodynamic coefficients of the complex-shaped autonomous underwater vehicle TUNA-SAND. *J. Mar. Sci. Technol.*, vol. 14, no. 3, pp. 373–386, 2009.
[8]. Ting G., Yaxing W., Yongjie P. & Jian C., Hull shape optimization for autonomous underwater vehicles using CFD, *Engineering Applications of Computational Fluid Mechanics (2016)*
[9]. Tyagi A. and Sen D., "Calculation of transverse hydrodynamic coefficients using computational fluid dynamic approach, *Ocean Eng., vol. 33, pp. 798–809, Apr. 2006*.

Nomenclature

r = The radial coordinate(mm)
v_x, v_r= The axial and radial velocity respectively(m/s)
S_m = The source term
ρ = Density of fluid (m^3/s)
v = Velocity of Autonomous Underwater vehicle(m/s)
τ_w = Wall Shear Stress (N/m^2)
C_f , C_d = Skin Friction Coefficient & Coefficient of Drag
θ = Hull tail semi-angle
a= Nose length(mm), b= Mid-section length(mm), c= Tail length(mm)
F_r, Fx= Radial & axial external body forces